Published by IOP Publishing for Sissa Medialab

Received: *September 29, 2025*
Accepted: *November 27, 2025*
Published: *December 10, 2025*

Tests of charge sharing compensation algorithm implemented in a single pixel counting integrated circuit operating with Si and CdTe pixel detectors

M. Zoladz[a,*] **P. Otfinowski**[a] **P. Grybos**[a] **R. Kleczek**[a] **and G. Deptuch**[a]

[a] *AGH University of Krakow,*
al. A. Mickiewicza 30, 30-059 Krakow, Poland

E-mail: zoladz@agh.edu.pl

Abstract: This study addresses the challenge of charge sharing in hybrid pixel detectors with small pixel pitches. In such detectors, charge generated by a single photon is distributed across adjacent pixels, leading to spectral distortion and degraded energy resolution in single-photon counting (SPC) mode. The paper evaluates the MPIX readout chip equipped with the charge sharing compensation algorithm, implemented both in analog and digital domains, to recover and correctly assign shared charge signals. The MPIX chip features a 96×192 — pixel matrix with four energy thresholds and inter-pixel communication, facilitating charge summation among neighboring pixels. The effectiveness of the algorithm was experimentally validated through measurements with CdTe and Si pixel sensors using monochromatic X-rays from fluorescence and radioactive sources, continuous-spectrum X-rays, and precisely controlled laser-induced charge injections. Results demonstrate a significant reduction of spectral distortions caused by charge sharing, and improved energy assignment accuracy. The tests with laser pulses were performed with the frequency range up to 12 MHz. The study confirms that the charge sharing compensation algorithm effectively reconstructs photon energy and assigns events to single pixels, enhancing hybrid pixel detector performance.

Keywords: Electronic detector readout concepts (solid-state); Front-end electronics for detector readout; VLSI circuits

*Corresponding author.

https://doi.org/10.1088/1748-0221/20/12/P12015

2025 JINST 20 P12015

Contents

2025 JINST 20 P12015

1 Introduction

1.1 Charge sharing in pixel detectors

Advancements in semiconductor technology have enabled development of hybrid pixel detectors with increasingly smaller pixel pitches. However, reducing pixel dimensions can impair detector performance as a result of increased charge sharing. Charge sharing is the process of distributing the charge generated by a single photon interaction among adjacent pixels, rather than collecting it fully in a single pixel.

In the single-photon counting (SPC) mode, detectors only register events when the signal amplitude exceeds a predefined threshold. A typical signal processing chain (figure 1(a)) includes a charge-sensitive amplifier (CSA), which converts the collected charge from the current to voltage domain. Then the signal is processed by a shaper and compared against a threshold voltage Vt by a discriminator. Digital pulses are generated when the threshold is exceeded and are counted over a defined time period, enabling photon rate measurements.

By scanning the discriminator's threshold across a range of voltages, an integral energy spectrum can be constructed. For a monochromatic source and full charge collection within a single pixel, this approach allows for accurate photon energy determination (figure 1(b)). However, when charge is shared between pixels — particularly when the interaction occurs near a pixel border (figure 1(c)) — the measured signal in each pixel may fall below the threshold. This effect leads to reduction in counts at the true photon energy and a translates to a false increase of counts when thresholds are lowered. The latter yields presence of lower-energy photons (figure 1(d), dashed line) that does not correspond with the impinging radiation. Such distortions degrade both spectral fidelity and energy resolution [1–3].

This work presents measurements performed using the MPIX readout chip bump-bonded to both CdTe and Si sensors. The chip incorporates charge-sharing compensation algorithms, whose effectiveness is evaluated by measurements both with X-ray sources and laser and discussed in details.

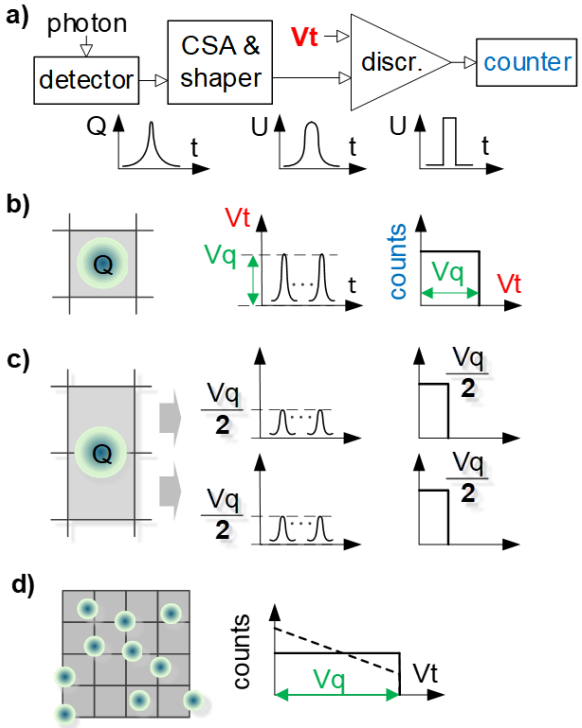

Figure 1. Charge sharing phenomena illustration: (a) Single photon counting signal processing path. (b) Integral energy scan. (c) Charge sharing. (d) Integral energy scans affected by charge sharing.

1.2 MPIX IC architecture with Multithreshold Pattern Recognition charge sharing compensation algorithm

The MPIX IC is designed in CMOS 130 nm technology, and its core consists of a matrix of 96×192 square-shaped pixels with a pitch of 100 µm [4] (figure 2(a)). Each pixel operates in the SPC mode and is equipped with the CSA, the shaper, four discriminators, and four 14-bit ripple counters per pixel (figure 2(b)). This architecture allows setting of four independent energy thresholds (VT0–VT3), which are configured globally for all 18,432 pixels within the matrix. To accommodate a wide range of applications(e.g. diffractometry measurements, food and security scanning, etc.), the MPIX IC provides eight configurable gain settings (controlled by CSA and shaper feedback capacitor) and is capable of processing X-ray photons with energies up to 154 keV. At the highest gain setting, the measured equivalent noise charge (ENC) is 123 e^- rms, with a linear response range extending up to approximately $E = 46$ keV when coupled to a CdTe detector. At the lowest gain setting, the ENC increases to 192 e^- rms, while the linear range extends up to $E = 154$ keV. The standard deviation of the pixel-to-pixel offset spread is reduced to 1 mV using trimming digital-to-analog converters. Under the nominal bias condition, the chip power consumption is 1.4 W.

The MPIX chip also supports an inter-pixel communication mode designed to reduce the impact of charge sharing. The Multithreshold Pattern Recognition (MPR) charge sharing compensation algorithm, previously described and theoretically simulated in [5], is implemented in this chip. This algorithm operates in both the analog and digital domains. In the analog domain, it facilitates the recovery of the full charge shared among neighboring pixels. Pre-amplified signals from four adjacent pixels are summed at the input of the shaper via coupling capacitors (Cc0–Cc3, see figure 2). The

2025 JINST 20 P12015

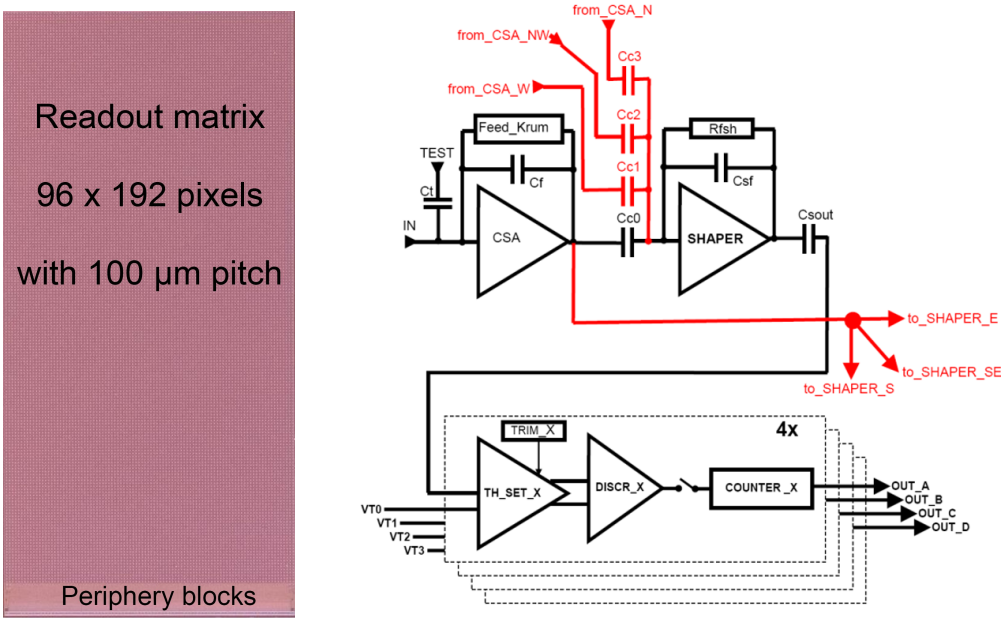

Figure 2. a) Photo of MPIX IC — chip size 9.6 mm × 20.3 mm, (b) Simplified scheme of a single pixel.

process of summing signals from four adjacent pixels is referred as occurring in a Signal Rebuild Hub (SRH). The resulting signal is then amplified and fed into the discriminators. This configuration enables reconstruction of the original amount of charge when the signal from a single photon is distributed across up to four readout channels. It is important to note that the analog front-end gain differs between the standard SPC mode and the MPR mode of operation.

In the digital domain, the algorithm associates the reconstructed photon's energy to one of four ranges, determined by the thresholds 0–3. The event is assigned to a single pixel and registered by the counter corresponding to the detected energy range. The operation of the algorithm steps through a few phases. Figure 3(a) shows an example of a charge shared event, where the intensity of color corresponds to amount of the collected charge. For the purpose of this example, we assumed an idealized charge sharing model [6], where Gaussian-shaped charge cloud is assumed and the final cloud size at the electrodes is determined by the detector parameters, such as the sensor thickness d, the depth of photon interaction depth λ, the bias voltage V, and is given by the equation:

$$\sigma = \sqrt{2kT\,(d-\lambda)^2\,/qV} \tag{1.1}$$

where $k = 1.38 \cdot 10^{-23}\,\mathrm{J{\cdot}K^{-1}}$ is the Boltzmann constant, $T = 300\,\mathrm{K}$, and $q = 1.602 \cdot 10^{-19}\,\mathrm{C}$ is the unit charge.

In the initial phase, the algorithm consolidates adjacent SRHs that have crossed the lowest discrimination threshold into a single cluster. Secondly, depending on the number of SRHs that cross a given threshold within this cluster, one threshold is selected for allocation, resulting in a pattern visible in figure 3(b). Subsequently, the Pattern Recognition [5] algorithm is executed, which fills the missing corners in the top-left direction and ultimately identifies the pixel located at the top-left corner of the obtained cluster and this pixel get the event assigned to (figure 3(c)). The energy of the photon is determined based on the SRH with the highest energy within the cluster.

2025 JINST 20 P12015

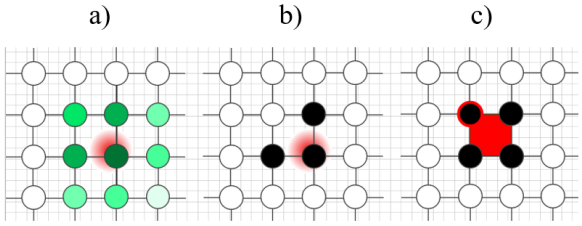

Figure 3. Pattern recognition sharing compensation algorithm illustration. (a) Charge rebuilding. (b) Charge discrimination. (c) Pixel selection.

2 Tests of the MPIX IC bump-bonded to pixel detectors

2.1 X-ray measurements with CdTe detector

To validate the charge sharing compensation algorithm using monochromatic X-rays, we employed both X-ray fluorescence (XRF) and monochromatic radioactive sources. Integral spectra were acquired with the charge sharing compensation algorithm both enabled and disabled, using the MPIX IC connected to 100 µm-pitch CdTe pixel detectors with a thickness of 750 µm.

For the XRF measurements, Molybdenum (Mo — 17.48 keV) and Silver (Ag — 22.16 keV) targets were used. In both cases, the characteristic distortions of the integral spectra caused by charge sharing were observed (see section 1.1, figure 1(c)). This distortion was corrected by switching the charge sharing compensation algorithm on (figure 4).

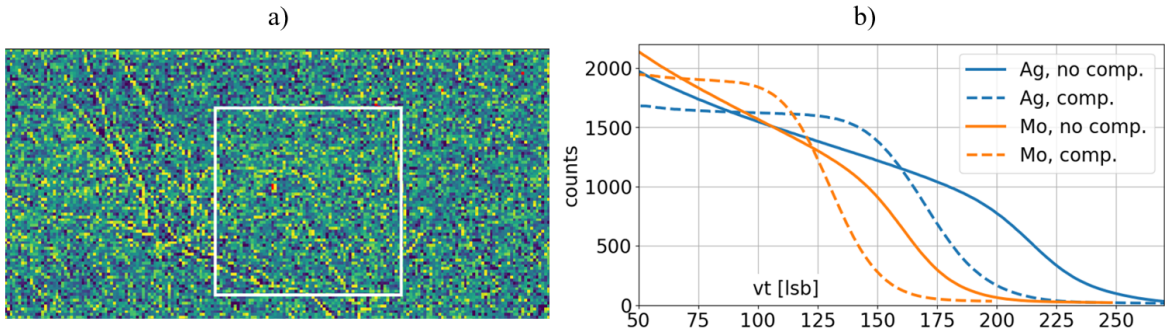

Figure 4. Measurements done with 0.75 mm thick CdTe detector module and illuminated by fluorescence X-rays from Ag target and Mo target (separately). (a) Distribution of counts across the pixel matrix. The measured integral spectra from the pixels within the white box were summed. (b) Integral spectra acquired with charge sharing compensation disabled and enabled.

In order to evaluate the MPR algorithm at higher photon energies, the same methodology was applied using monochromatic radioactive sources commonly employed for nuclear calibration. Specifically, Am-241 and Cd-109 sources were utilized in this study.

The sources were positioned a few millimeters from the detector's surface (figure 5). For both sources, distortion in the integral spectra was observed due to charge sharing, as well as its mitigation following the application of the charge sharing compensation algorithm (figure 6). In the case of Am-241, both the primary and weaker gamma emission lines were detected; however, the weaker lines were not clearly distinguishable. For Cd-109, the main gamma line was identified, accompanied by the distinctive X-ray line that results from subsequent electron capture.

2025 JINST 20 P12015

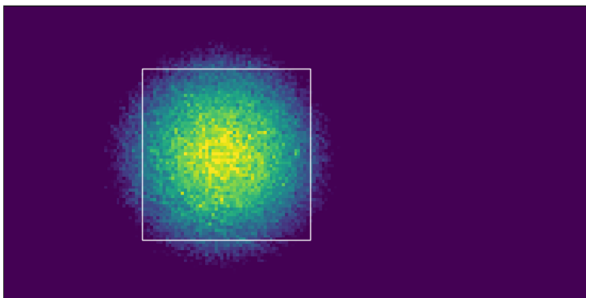

Figure 5. Counts distribution acquired by CdTe 0.75 mm detector's module generated by Am-214 monochromatic radioactive source placed on the detector module. The measured integral spectra from the pixels within the white box were summed and are presented in the figure 6.

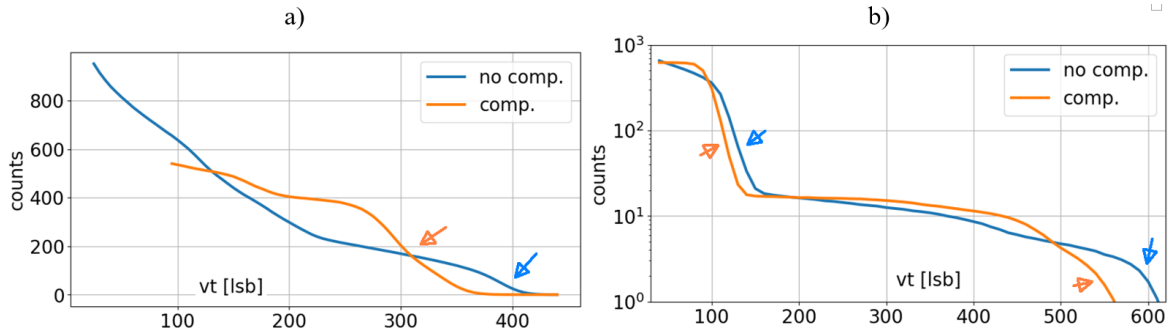

Figure 6. Integral spectra of X-rays from monochromatic radioactive sources for charge sharing compensation disabled and enabled. (a) Am-241 (main gamma line 59.54 keV). (b) Cd-109 (main gamma line 88.03 keV and 25 keV from electron capture Silver $K_{\beta 1}$).

The evaluation of the charge sharing compensation algorithm was also conducted using continuous-spectrum X-rays, which are frequently utilized in medical imaging and industrial applications, such as food inspection systems (figure 7). To this end, two distinct X-ray tubes were utilized, operated at a different voltages 60 kVp and 130 kVp. While the interpretation of the results is more challenging in comparison with the case of monochromatic X-rays, it is evident that the charge sharing compensation algorithm reduces the number of counts erroneously assigned to lower energies, redistributing them toward higher energy regions of the spectrum.

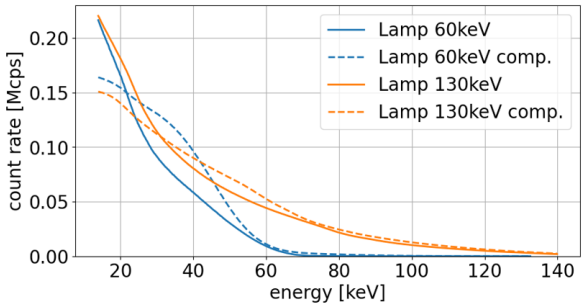

Figure 7. Integrated threshold scans of radiation from 60 kVp and 130 kVp X-ray tube with charge sharing compensation disabled and enabled.

2025 JINST 20 P12015

2.2 Laser measurements with Si detector

In order to experimentally verify the charge sharing compensation algorithm, the 400 µm-thick, 100 µm-pitch, p-type Si pixel detector bump-bonded to the MPIX IC was illuminated using an infrared femtosecond laser (Calmar OPP-UTF01, λ = 1060 nm). The experimental setup enables the laser beam to be focused on a small group of pixels and to generate short pulses at the repetition rates ranging from a few kHz up to 12 MHz.

In comparison with X-ray sources, laser-induced charge injections are repeatable and yield well-controlled charge distributions. This enables the algorithm to be verified in a step-by-step manner with single-pixel resolution. In contrast, photons from real X-ray sources interact with the detector at random locations, forcing to rely on statistical analysis instead of being able to study specific charge sharing scenarios that can be obtained in lateral scan the detector surface by the laser beam.

Figures 8–10 present the results of measurements obtained with the laser beam focused on the same location, ensuring an identical charge distribution, while varying the internal chip configuration. Figure 8(a) shows the integral spectra acquired with signal summing disabled, corresponding to the standard (SPC) mode. Figure 8(b) displays the spectra obtained with signal summing enabled. Figure 8(c) overlays the spatial charge distribution maps for both configurations: the black font represents measurements with signal summing disabled, while the red font corresponds to signal summing enabled.

The results confirm that the highest reconstructed charge sum (756) is observed at the signal-receiving hub (SRH), which is surrounded by pixels registering high individual charges (186, 294, 347, and 273), illustrating the correct identification and summation of shared charge contributions.

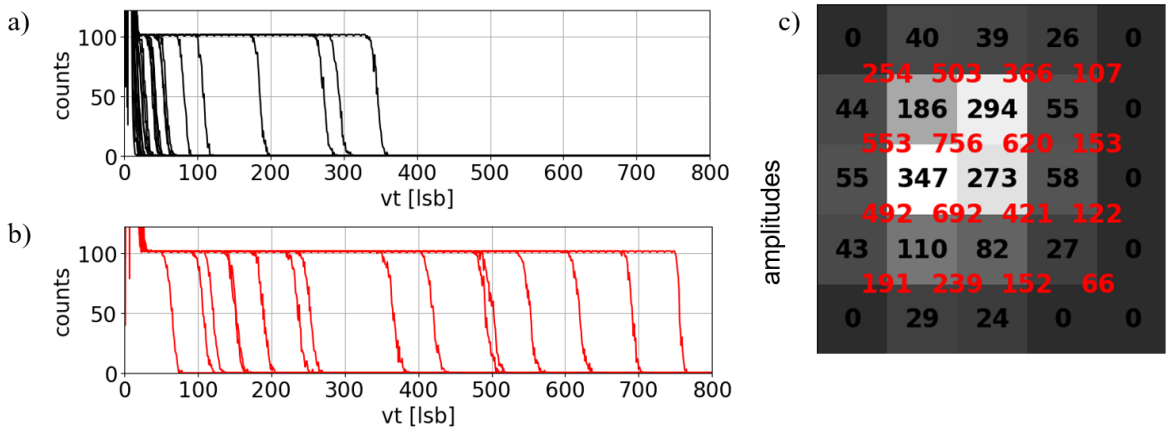

Figure 8. Integral spectra acquired with signal summing disabled (a) and enabled (b). (c) Signal amplitudes distribution with signal summing disabled (black font) and enabled (red font).

Figure 9(a) presents the integral spectra acquired with signal summing enabled, with the discrimination threshold level indicated in green. Figure 9(b) illustrates the corresponding spatial distribution of signal amplitudes, where pixels that exceed the discrimination threshold are highlighted with green frames. These pixels form a cluster, within which the top-left pixel would be selected as the "winner" by the pattern recognition algorithm, if enabled (see section 1.2, figure 3).

As illustrated in figure 9(c), the number of registered counts as a function of the discrimination threshold, with the pattern recognition algorithm enabled. As illustrated in figure 9(c), the number of

2025 JINST 20 P12015

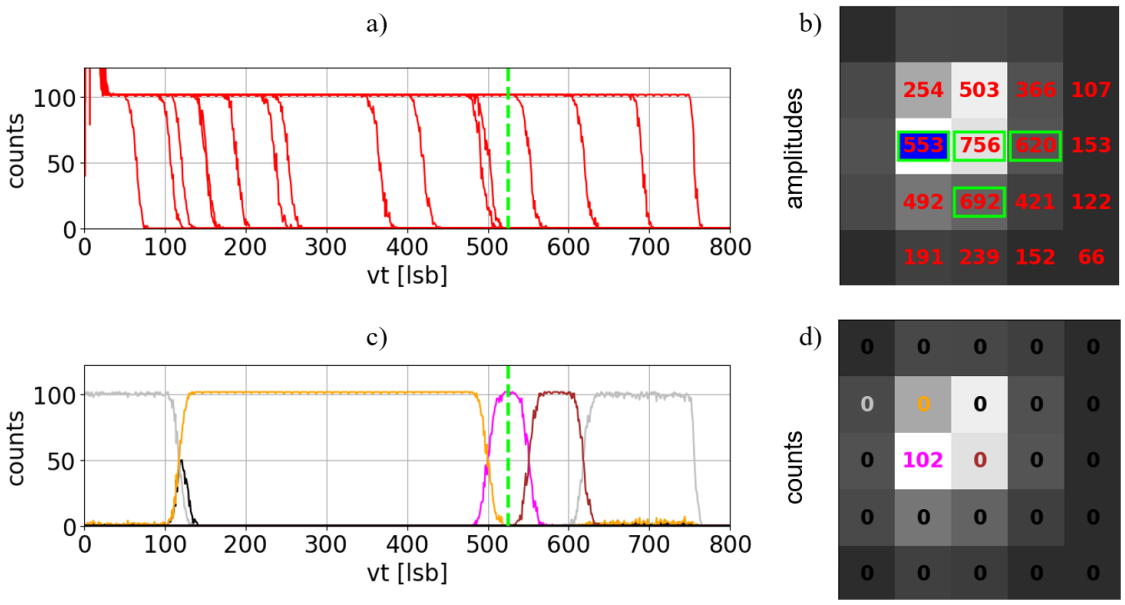

Figure 9. Results of measurements with signal summing enabled: (a) SRHs integral spectra with discrimination level equal to 525 (green line) (b) SRHs amplitude distribution with highlighted pixels crossing discrimination threshold (green frames) and an expected winner (blue filled frame). Results of measurements with MPR algorithm enabled: (c) Number of registered counts with discrimination level marked (green line), (d) counts distribution for highlighted discrimination level.

registered counts is shown as a function of the discrimination threshold with the pattern recognition algorithm enabled. The results demonstrate that the algorithm's decision is threshold-dependent; that is to say, the 'winning' pixel position depends on the threshold. However, each event is consistently registered by a single pixel only. As illustrated in figure 9(d), the spatial distribution of counts for a selected threshold level. Only one pixel records events specifically, the pixel that exhibited the highest signal amplitude in the conventional SPC mode confirming the correct allocation by the algorithm.

Figure 10 presents the same type of measurement as shown in figure 9, but with a different discrimination threshold applied. It can be noticed that the event is now allocated to a different pixel. This highlights the critical importance of selecting an appropriate discrimination level to ensure correct signal allocation by the pattern recognition algorithm.

We also measured the count rate as a function of the laser pulse frequency. Unlike monochromatic radioactive sources, which follow Poisson distribution and are more prone to causing pulse pile-up in the signal processing chain, the laser provides a uniform temporal distribution of charge pulses. However, the test with a laser allows us to gain insight into the system's behavior as the input pulse frequency increases.

For both non-compensation and the charge sharing compensation modes, the integral spectra showed a decrease in pulse amplitude with increasing laser frequency (figure 11(a), figure 12(a)). However, no significant reduction in count rate was observed up to 12 MHz when the discrimination threshold was set to a value corresponding to half the photon energy (figure 11(b) and figure 12(b)). This indicates that the system maintains full event registration efficiency up to this frequency under these threshold conditions. It is noteworthy that the shape of the integral spectra in the compensation mode confirms that counts are allocated to only one pixel for the specified discrimination threshold (figure 12(a)).

2025 JINST 20 P12015

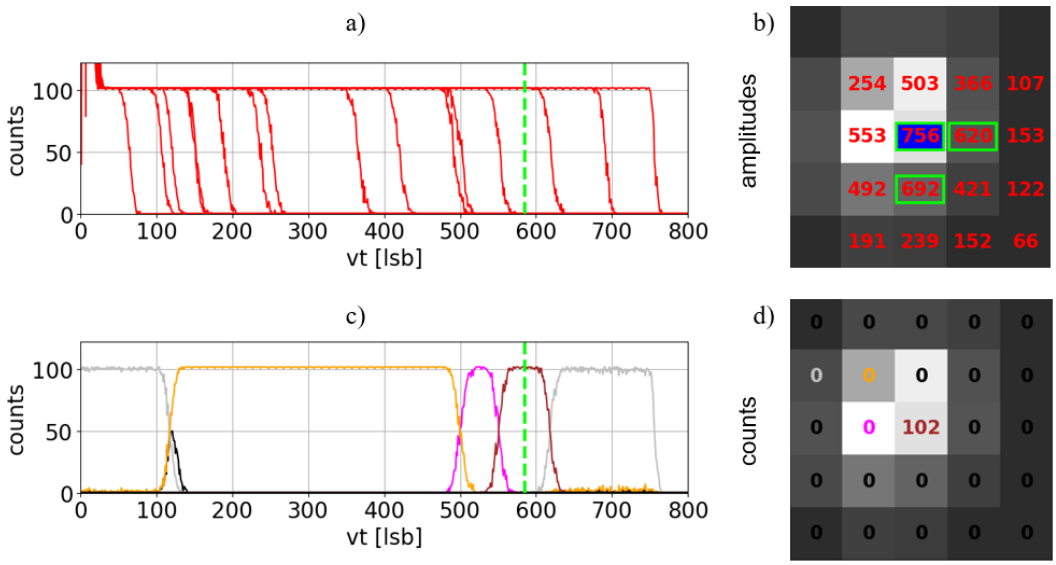

Figure 10. Results of measurements with signal summing enabled: (a) SRHs integral spectra with discrimination level equal to 585 (green line). (b) SRHs amplitude distribution with highlighted pixels crossing discrimination threshold (green frames) and an expected winner (blue filled frame). Results of measurements with MPR algorithm enabled: (c) Number of registered counts with discrimination level marked (green line), (d) counts distribution for highlighted discrimination level.

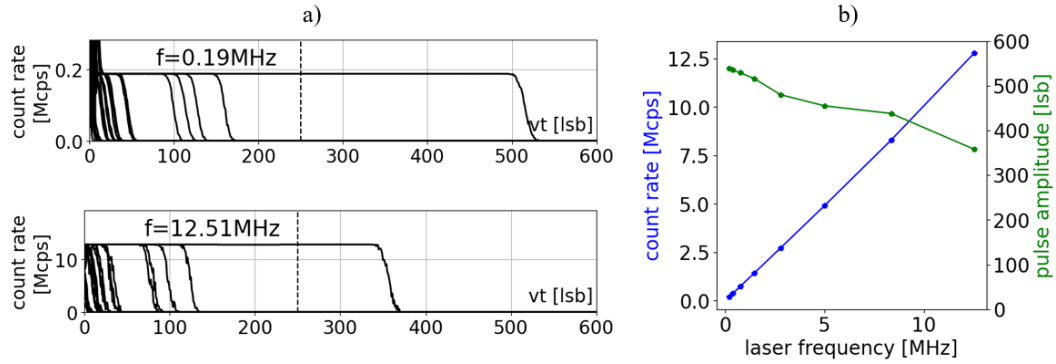

Figure 11. Count rate and pulse amplitudes vs. laser pulses frequency measured without charge sharing compensation. (a) Integral spectra. (b) Count rate and pulse amplitude in terms of laser pulses frequency.

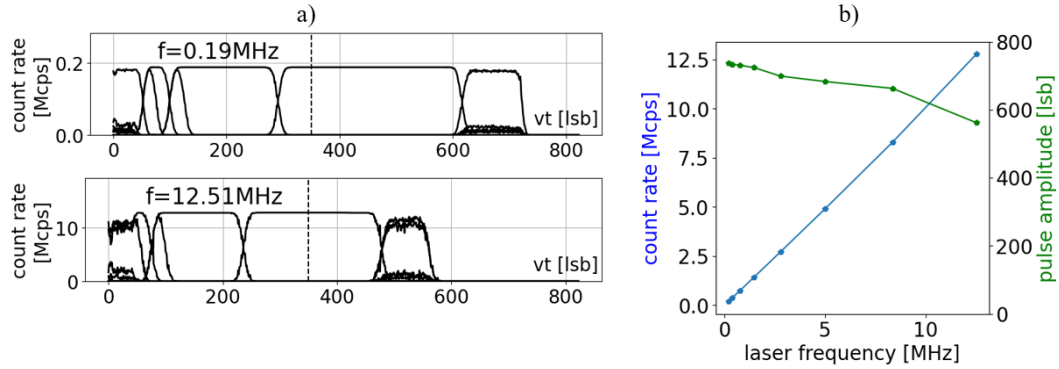

Figure 12. Count rate and pulse amplitudes vs. laser pulses frequency measured with charge sharing compensation. (a) Number of registered counts. (b) Count rate and pulse amplitude in terms of laser pulses frequency.

2025 JINST 20 P12015

3 Summary

In this paper, we presented a systematic validation of the pattern recognition algorithm for charge sharing compensation in pixel detectors. Low-energy monochromatic X-rays produced via X-ray fluorescence (XRF) using Molybdenum (Mo) and Silver (Ag) targets (17.480 keV and 22.163 keV, respectively) were employed to investigate the algorithm's effectiveness. The integral spectra clearly demonstrated the presence of charge sharing in the case of the algorithm disabled, and effective charge sharing compensation when enabled. Similar confirmation was achieved at higher energies (59.54 keV and 88.03 keV) using Am-241 and Cd-109 radioactive sources.

Additionally, charge sharing compensation was evaluated with continuous X-ray spectra generated by tubes operated at 60 kVp and 130 kVp. Although the interpretation of these results is more complex, the observed reduction in counts assigned to lower energies in favor of higher energy counts provides strong evidence of successful charge sharing compensation.

Finally, by illuminating the detector with focused laser pulses at a constant frequency, we generated stable and repeatable charge distributions across multiple adjacent pixels. A comparative analysis of measurements acquired with no compensation, signal summing only, and both signal summing and pattern recognition enabled confirmed that photon hits were correctly allocated to a single, appropriate pixel.

Acknowledgments

This work is supported by the National Science Centre, Poland, project no. 2023/51/B/ST7/01782.

References

[1] R. Ballabriga et al., *Review of hybrid pixel detector readout ASICs for spectroscopic X-ray imaging*, 2016 *JINST* **11** P01007.

[2] A. Krzyżanowska et al., *Characterization of the Photon Counting CHASE Jr., Chip Built in a 40-nm CMOS Process With a Charge Sharing Correction Algorithm Using a Collimated X-Ray Beam*, *IEEE Trans. Nucl. Sci.* **64** (2017) 2561.

[3] G.W. Deptuch et al., *An Algorithm of an X-ray Hit Allocation to a Single Pixel in a Cluster and Its Test-Circuit Implementation*, *IEEE Trans. Circuits Theor.* **65** (2017) 185.

[4] P. Grybos et al., *Hybrid Detector with Interpixel Communication for Color X-ray Imaging*, in the proceedings of the *28th IEEE International Conference on Electronics, Circuits, and Systems (ICECS)*, Dubai, UAE, November 28–December 1 (2021) [DOI:10.1109/icecs53924.2021.9665489].

[5] P. Otfinowski, A. Krzyżanowska, P. Gryboś and R. Szczygieł, *Pattern recognition algorithm for charge sharing compensation in single photon counting pixel detectors*, 2019 *JINST* **14** C01017.

[6] G. Lutz, *Semiconductor Radiation Detectors*, Springer Berlin Heidelberg (2007) [DOI:10.1007/978-3-540-71679-2].

2025 JINST 20 P12015